DEFINING HEPATIC MODIFIERS OF ATTR AMYLOIDOSIS THROUGH THERAPEUTIC GENE EDITING IN PATIENT IPSCS

Richard M. Giadone[1], Derek C. Liberti[1], Taylor M. Matte[1], Nicholas Skvir[1], Kai-Chun Chen[3], J.C. Jean[1,2], Andrew A. Wilson[1,2], Darrell N. Kotton[1,2], R. Luke Wiseman[3], George J. Murphy[1,4]

[1]Center for Regenerative Medicine, Boston University School of Medicine, Boston, MA, USA.

[2]The Pulmonary Center and Department of Medicine, Boston University School of Medicine, Boston, MA, USA.

[3]Department of Molecular Medicine, The Scripps Research Institute, La Jolla, CA, USA.

[4]Section of Hematology and Oncology, Department of Medicine, Boston University School of Medicine, Boston, MA, USA.

*Correspondence: gjmurphy@bu.edu, Center for Regenerative Medicine, 670 Albany Street, 2nd Floor, Boston, MA 02118, USA.

Running title: Gene editing ATTR amyloidosis iPSCs

Key Words: hereditary amyloidosis, pluripotent stem cells, gene editing, single cell transcriptomics, hepatic disease

ABSTRACT

Hereditary transthyretin amyloidosis (ATTR amyloidosis) is a multi-system, autosomal dominant protein folding disorder that results from over 100 described mutations in the transthyretin (*TTR*) gene. Here, we employed a universal gene editing strategy in patient-specific, induced pluripotent stem cells (iPSCs) that allows for the amelioration of all *TTR* genetic lesions, thereby eliminating the production of destabilized, disease-causing variants. Mass spectrometric analysis of corrected iPSC-derived hepatic supernatants revealed elimination of mutant TTR, resulting in diminished neuronal target cell toxicity. This procedure also allowed for the interrogation of global transcriptomic differences between control iPSC-derived hepatocyte-like cells (HLCs) and those expressing the most proteotoxic disease-causing TTR mutation. By employing single cell RNA sequencing (scRNAseq) to compare syngeneic corrected and uncorrected ATTR amyloidosis iPSC-derived HLCs, we found distinct transcriptional changes in cells expressing the disease-associated TTR mutant, including activation of unfolded protein response (UPR)-associated signaling pathways shown to protect the extracellular space from proteotoxic TTR aggregation. Results from these studies represent a potential cell-based therapeutic strategy for treating all forms of ATTR amyloidosis and challenge the notion that ATTR livers are unaffected in disease pathogenesis, highlighting possible biomarkers for this notoriously difficult to diagnose disease.

INTRODUCTION

Systemic amyloidosis represents a class of disorders characterized by the misfolding of endogenous proteins that results in the formation of proteotoxic species at downstream target organs. These disorders, encompassing over 20 structurally distinct proteins, affect >1 million individuals worldwide (1-4). One such disease, hereditary transthyretin amyloidosis (ATTR amyloidosis), is an autosomal dominant disorder that can result from over 100 possible mutations in the transthyretin (*TTR*) gene (5, 6). TTR is produced chiefly by the liver where it forms a homotetramer, allowing for transport of thyroxine and retinol binding protein throughout circulation. In patients with ATTR amyloidosis, TTR mutations decrease the stability of the tetramer and result in monomerization and

subsequent misfolding of TTR variants. Amyloid-prone monomers then aggregate to form proteotoxic low-molecular weight oligomers and, eventually, hallmark Congophilic amyloid fibrils. Toxic TTR species deposit extracellularly at downstream targets such as the peripheral nervous system and cardiac tissue, resulting in cellular damage (6-9).

Previous studies have demonstrated that the reduction of circulating levels of TTR results in decreased target organ toxicity. In line with this rationale, the current standard of care for patients with ATTR amyloidosis is orthotopic liver transplantation (10-13). Although effective, not all patients are candidates for surgery (due to age or disease progression), and massive donor organ shortages necessitate additional treatment options. Notably, the livers of ATTR amyloidosis patients have traditionally been thought to be unaffected throughout disease pathogenesis as toxicity occurs at downstream target organs (e.g., peripheral nerves and cardiac tissue). Highlighting this point, in order to cope with the scarcity of donor organs available for transplant, domino liver transplants (DLTs) are routinely performed in which the liver of an ATTR individual is removed and replaced via orthotopic liver transplantation, and subsequently given to an individual in end-stage liver failure (14). Coupled with the thinking that ATTR amyloidosis livers are otherwise normal, this methodology is allowable since the disease takes 5-6 decades to develop in an individual. However, recent studies show that DLT recipients develop TTR fibrils at target organs at a greatly accelerated rate, less than 10 years post-DLT, suggesting a hepatic driver in ATTR pathogenesis that accelerates disease progression in these transplant recipients (15-17). Other treatment alternatives are small molecules such as diflunisal and Tafamidis, which stabilize the tetrameric form of TTR in order to limit monomerization and fibril formation from occurring. While results from recent clinical trials suggest a decrease in ATTR-related mortality, not all patients respond equally and effectively to these treatments likely due to differences in genetic background (18-20). Similarly, experimental small interfering RNA species (siRNAs) are being developed to target and eliminate both wild-type *and* mutant TTR species (21). Although effective in this regard, recent studies show a number of neuronal cell types are capable of protective local TTR synthesis in instances of neuronal stress (22-24). Despite targeted delivery of these siRNAs to the liver, the

possibility for unintended side-effects mediated by the global reduction of TTR levels warrant further understanding of the protein in additional cell types.

ATTR amyloidosis is a complex genetic disease with wide-ranging penetrance and pathogenesis. Though considered a rare disease, ATTR amyloidosis is thought to be underdiagnosed due to the seemingly unrelated nature of initial presentation, highlighting the need for predictive biomarkers (25, 26). Due to the multi-tissue etiology and the age-related trajectory of the disease, ATTR amyloidosis has proven difficult to study in a physiologically relevant way. At the same time, no mouse model currently recapitulates key aspects of human ATTR pathology (27-30). To these ends, our laboratory has developed an induced pluripotent stem cell (iPSC)-based model for studying the disease (27, 28). Briefly, ATTR patient iPSCs are specified to effector hepatocyte-cells (HLCs) that secrete a destabilized, amyloidogenic TTR mutant. Peripheral target cells such as iPSC-derived neuronal lineages or SH-SY5Y cells can then be dosed with amyloid containing, iPSC-derived hepatic supernatant and resulting toxicity can be quantified.

Here, we utilize the inherent flexibility of our iPSC-based platform to develop a universal gene correction strategy ameliorative of all TTR genetic lesions. Using this approach, we show that selective replacement of the single *TTR* mutant allele with wild-type TTR reduces secretion of the mutant protein and decreases neuronal target cell toxicity. Furthermore, we use single cell RNA sequencing (scRNAseq) to define transcriptional changes in syngeneic corrected and uncorrected ATTR amyloidosis iPSC-derived HLCs. Through these efforts, we show that the presence of the destabilized, disease-associated TTR^{L55P} mutant in HLCs increases expression of genes and pathways previously linked to the toxic extracellular aggregation of TTR, including transferrin and unfolded protein response (UPR) target genes. Herein, we discuss the potential for our gene correction strategy as a universal, cell-based treatment for all forms of ATTR amyloidosis as well as discuss potential implications of altered hepatic expression of disease modifying factors in the extracellular aggregation and toxicity of TTR variants.

RESULTS AND DISCUSSION

TTR is a top differentially expressed gene throughout human hepatic specification.
Recent work from our group demonstrated the emergence of a stage-dependent hepatic signature through the temporal mapping of hepatic-specified pluripotent stem cells (PSCs) (31). In these experiments, microarray analyses were performed on cells isolated at days 0, 5, and 24 of hepatic specification. Interestingly, repurposing of this data revealed that *TTR* was the second most differentially expressed gene throughout the differentiation **(Fig. 1A)**. To confirm this, qRT-PCR was performed on RNA isolated from day 24 HLCs demonstrating significant, robust upregulation of *TTR* as compared to undifferentiated iPSCs **(Fig. 1B)**.

A universal gene editing strategy for hereditary amyloidosis and the creation of a TTR-driven, hepatic specification reporter iPSC line.
As ATTR amyloidosis results from over 100 described mutations in the *TTR* gene (5, 6), conventional site-specific gene editing techniques, requiring unique oligonucleotide targeting constructs, remain impractical and limit the feasibility of cell-based therapeutic strategies for the disease. As noted above, *TTR* is one of the most differentially expressed genes in hepatocyte differentiations, indicating that it would be an excellent candidate to target for a hepatic specification reporter iPSC line. To these ends, we hypothesized that the methodology we would employ to create this reporter could also serve as a singular, 'universal' gene correction strategy ameliorative of the >100 described ATTR amyloidosis-causing genetic lesions. To accomplish this, TALEN-mediated gene editing was used to manipulate an iPSC line derived from a patient with the Leu55 →Pro (TTR^{L55P}) mutation, the most proteotoxic disease-causing variant (27, 28). In order to implement a broadly applicable gene correction strategy, a wild-type copy of the *TTR* gene, fused to *eGFP* via a 2A self-cleaving peptide, was targeted to the transcriptional start site (TSS) of the endogenous, mutant *TTR* allele **(Fig 1C)**. Inclusion of a 2A peptide allows for transcription of a bicistronic mRNA containing independent open reading frames for *TTR* and *eGFP* that ultimately results in independent proteins via a post-translational cleavage event. As a result of this targeting methodology, transcription and translation of mutant TTR is blunted via introduction of an artificial STOP codon, and replaced with a wild-type copy of the gene **(Fig. 1C)**. After targeting

and selection of puromycin resistant colonies, the puromycin resistance ($puro^R$) and PGK cassettes were removed via transient expression of Cre recombinase and clonal populations were generated via single cell sorting. In order to identify clones in which the donor construct was inserted at the appropriate location in the *TTR* locus and the $puro^R$ cassette was removed, a genomic PCR screening strategy was performed (**Supplemental Figs. 1A, 1B**). IPSC lines were analyzed for karyotypic stability pre- and post-targeting (**Supplemental Fig. 1C**). Importantly, the universal gene correction strategy described here provides a singular technique for ameliorating all *TTR* genetic lesions while simultaneously obviating concerns regarding haploinsufficiency via replacement of the endogenous mutant *TTR* allele with a wild-type copy.

Using this established reporter line, we constructed a temporal map of GFP^+ (i.e. TTR^+) cells throughout HLC differentiation. TTR presented as an early hepatic marker, with expression peaking at approximately day 16 of a 24 day specification protocol **(Fig. 1D)**. By day 24 of the differentiation, HLCs exhibited cobblestone-like morphology reminiscent of primary hepatocytes, and the majority of cells expressed TTR **(Fig. 1E)**. To further validate this reporter line and ensure that GFP expression correlated with the expression of TTR as well as other hepatic-specification markers, day 16 GFP^+ HLCs were sorted and assayed via qRT-PCR. GFP^+ cells were found to be significantly enriched for *TTR*, as well as other hepatic specification markers such as *AAT* and *ALB* **(Fig. 1F),** suggesting that our 'corrected' TTR reporter cell line efficiently enriches for maturing hepatic-lineage cells during specification.

Gene-edited iPSC-derived HLCs no longer produce destabilized, disease-causing TTR variants.

Following the successful targeting and validation of our TTR-GFP fusion construct to the TSS of the TTR^{L55P} locus, we next examined the ability of this strategy to eliminate the production of destabilized, disease-causing TTR, as well as alleviate downstream neuronal toxicity **(outlined in Fig. 2A)**. To this end, wild-type, corrected, and 'uncorrected' (i.e. non-targeted, heterozygous TTR^{L55P}) iPSCs were differentiated into HLCs. Conditioned supernatant from each line was created by culturing cells for 72 hours in hepatic specification media. Supernatants were then collected, concentrated,

and interrogated via LC/MS for the presence of different TTR variants. As expected, wild-type hepatic supernatants were found to contain TTR^{WT} and no destabilized species. In contrast, uncorrected HLC supernatants produced from iPSCs heterozygous for the TTR^{L55P} mutation, contained TTR^{WT} and destabilized TTR^{L55P} variants. Remarkably, supernatant from corrected iPSC-derived HLCs revealed complete elimination of TTR^{L55P}, while levels of TTR^{WT} remained unperturbed, suggesting that the proposed gene correction strategy eliminated aberrant TTR while maintaining similar amounts of TTR^{WT} as observed in the control **(Fig. 2B)**. Importantly, the two amino acid overhang on the N-terminal portion of TTR, resulting from the post-translational cleavage of the 2A peptide, was removed with the TTR signal peptide through normal protein processing in the ER, resulting in TTR^{WT} from our donor construct that is indistinguishable from the endogenous form.

Decreased toxicity in neuronal cells dosed with corrected vs. uncorrected iPSC-derived HLC supernatants.

Many studies have shown that decreasing circulating levels of destabilized TTR species, as in the case of liver transplantation and our novel gene editing strategy, results in decreased peripheral organ dysfunction (10-13). As such, we sought to determine the efficacy of our iPSC-based gene correction methodology in decreasing target neuronal cell toxicity in our cell-based model. To accomplish this, a neuroblastoma (SH-SY5Y) cell line was dosed with conditioned supernatant generated from wild-type, uncorrected, or corrected iPSC-derived HLCs and surveyed for toxicity. In these assays, SH-SY5Y cells dosed with uncorrected hepatic supernatant displayed an increase in PI^{+} cells compared to those dosed with wild-type supernatant **(Fig. 2C)**. Cells dosed with corrected supernatant, however, exhibited a decrease in toxicity comparable to levels observed in the wild-type condition **(Fig. 2C)**. These results suggest that the proposed gene correction strategy successfully ameliorates TTR-mediated neuronal toxicity via elimination of toxic TTR production. Although the pathology of ATTR amyloidosis has been well characterized, the molecular mechanisms underlying disease-specific cell death remain elusive. Future studies will aim to identify signatures of cellular stress and damage in response to destabilized TTR species in

order to develop a more nuanced disease signature across multiple target cell types. Although the utility of gene editing-based therapies for liver-derived diseases is dependent upon future technical advancements, recent studies demonstrating the engraftment of PSC-derived hepatic cells in the livers of mice provide proof-of-principle for this strategy (32).

Single cell RNA sequencing comparing TTR^{L55P} and corrected syngeneic iPSC-derived HLCs reveals a novel hepatic gene signature.

Historically, it was thought that the livers of patients with ATTR amyloidosis are unaffected during disease pathogenesis (13, 33, 34). However, recent work calling into question the use of donor organs from ATTR amyloidosis patients for DLT procedures challenges this notion (15-17, 35, 36). Furthermore, recent evidence highlights a significant potential role for the liver in regulating the extracellular aggregation and distal deposition of TTR implicated in ATTR disease pathogenesis (7, 37). Collectively, these results indicate that genetic or aging-related perturbations to the liver could exacerbate the toxic extracellular aggregation and deposition of TTR aggregates on peripheral target tissues.

In order to define specific hepatic proteins and pathways important for regulating the secretion of destabilized, amyloidogenic TTR variants, we coupled our TTR reporter system with single cell RNA sequencing (scRNAseq) to compare mRNA expression profiles in syngeneic iPSC-derived HLCs with or without the TTR^{L55P} mutation. In addition to our corrected TTR reporter iPSC line, we also constructed a reporter cell line where our TTR-GFP donor construct was targeted to the wild-type TTR allele in the same TTR^{L55P} parental iPSC line. In effect, in contrast to our *corrected* reporter line, in our *uncorrected* reporter system, the TTR-GFP fusion construct disrupts the wild-type allele, leaving the mutant allele intact. As a result, we created two independent, TTR-promoter driven hepatic-specification reporter iPSC lines in isogenic backgrounds, where the only difference is the presence or absence of the TTR^{L55P} mutation. To compare HLCs +/- TTR^{L55P}, uncorrected and corrected reporter iPSCs were subjected to our hepatic specification protocol until TTR expression was maximal (day 16 of the differentiation) **(Fig. 1D)**. To control for the inherent heterogeneity of iPSC

differentiations, GFP^+ (TTR^+) cells were sort-purified to select for cells at identical stages in their developmental trajectories. Transcriptomic profiling was subsequently performed at single cell resolution via the Fluidigm C1 platform **(outlined in Fig. 3A)**.

Remarkably, uncorrected and corrected day 16 HLCs clustered independently of one another by principal component analysis (PCA) **(Fig. 3B)**. This differential clustering reflected a distinct transcriptional signature that distinguished corrected from uncorrected HLCs, with 92 genes being differentially expressed between the conditions **(Fig. 3C, 3D, Supplemental Data File 1)**. Genes showing increased expression in uncorrected cells could reflect specific proteins or pathways whose activity could enhance or inhibit the pathologic TTR extracellular aggregation associated with ATTR disease pathogenesis. Interestingly, our analysis identified the increased expression of two distinct genes/pathways previously shown to influence extracellular aggregation of destabilized TTRs (vide infra) (38-42).

Transferrin expression is significantly increased in uncorrected iPSC-derived HLCs and may represent a novel biomarker of disease.

The top differentially expressed gene in TTR^{L55P} expressing HLCs is the iron transporter, transferrin (TF) (**Fig. 3C, 3D**). Although TF is a marker of hepatic specification, no other hepatic marker, including *TTR*, is differentially expressed in corrected or uncorrected HLCs, indicating that the differential expression of *TF* is not due to the differentiation status of individual lines (**Fig. 3D** and **Supplemental Fig. 2**). Interestingly, a number of studies have implicated TF in the pathogenesis of other amyloid disorders such as Alzheimer's Disease (AD). One study, for example, demonstrated increased protein-level expression of TF in the prefrontal cortices of AD patients compared to elderly, non-diseased individuals (43). Recent work has identified physical interactions between TF and amyloid ß peptide (Aß), the amyloidogenic protein species in AD (44, 45). Furthermore, it has been demonstrated that TF plays a potential therapeutic role in AD tissues, preventing self-assembly and resulting toxicity of Aß oligomers (45).

Iron has been shown to increase in a number of organs throughout aging (46-48). As Congophilic TTR fibrils form in patients after 5-6 decades, pathogenesis of

ATTR amyloidosis is considered to have a strong aging-related component (7). At the same time, *in vivo* data has demonstrated physical interactions between TF and TTR amyloid fibrils (49). These observations, together with our scRNAseq data, suggest the possibility that TF plays a similar protective role in ATTR amyloidosis. In this model, hepatic cells producing mutant TTR may express higher levels of TF to prevent toxicity or fibril formation. As the availability of iron-free TF decreases with age, the anti-amyloid capacity of TF could be diminished, and as a result, TTR amyloid fibrils could form more readily, and ultimately lead to disease manifestation. At the same time, these observations raise the possibility that TF (or other orthogonal metabolites) could serve as a predictive biomarker for ATTR amyloidosis and thus aid in the treatment of this notoriously difficult to diagnose disease.

Uncorrected iPSCs show increased activation of protective UPR signaling pathways. Apart from *TF*, our scRNAseq analysis also identified increased expression of multiple ER proteostasis factors (e.g., *HYOU1* and *EDEM2*) in iPSC-derived HLCs expressing TTR^{L55P}. These genes have important roles in regulating proteostasis within the ER. In addition, transcription of these factors is regulated in response to ER stress as part of the unfolded protein response (UPR) – a tripartite ER stress-responsive signaling pathway responsible for maintaining proteostasis within the ER and throughout the secretory pathway (50, 51). Thus, the increased expression of these ER proteostasis factors suggests that the presence of the destabilized TTR^{L55P} protein challenges the ER proteostasis environment and activates the UPR.

Interestingly, ER stress and UPR activation can influence the toxic extracellular aggregation of amyloidogenic TTR mutants implicated in ATTR disease pathogenesis. Chemical toxins that induce severe, unresolvable ER stress in mammalian cells decrease the population of amyloidogenic TTR secreted as the native TTR tetramer and instead increase TTR secretion in non-native conformations that rapidly aggregate into soluble oligomers implicated in ATTR disease pathogenesis (38). In contrast, enhancing ER proteostasis through the stress-independent activation of the adaptive UPR-associated transcription factors ATF6 selectively reduces the secretion and subsequent aggregation of destabilized, amyloidogenic TTR variants (39-42). This suggests that

activation of adaptive UPR signaling pathways independent of severe ER stress can be a protective mechanism to suppress the secretion and toxic aggregation of destabilized, amyloidogenic TTR mutants.

In order to better define the impact of TTR^{L55P} expression on ER stress and UPR activation, we used gene set enrichment analysis (GSEA) to define the extent of UPR pathway activation in our uncorrected iPSC-derived hepatic lineages. The UPR consists of three integrated signaling pathways activated downstream of the ER stress-sensing proteins IRE1, ATF6, and PERK (50, 51). The activation of these pathways ultimately results in the activation of UPR-associated transcription factors including XBP1s (activated downstream of IRE1), ATF6 (a cleaved product of full length ATF6), and ATF4 and CHOP (two transcription factors activated downstream of PERK)(50, 51). These transcription factors induce overlapping, but distinct sets of stress-responsive genes, allowing their activation to be followed by specific transcriptional signatures. We used published transcriptional profiles for each of these three signaling pathways to establish IRE1-, ATF6-, and PERK-regulated genesets that allowed us to define their activation in HLCs using GSEA (42, 52). Notably, this analysis revealed modest activation of the adaptive IRE1/XBP1s and ATF6 transcriptional signaling pathways, with no significant activation of the PERK pathway. This indicates that the expression of TTR^{L55P} in iPSC-derived HLCs does not induce severe ER stress and suggests that the activation of adaptive IRE1/XBP1s and ATF6 signaling observed in these cells reflects a protective mechanism to suppress secretion and subsequent aggregation of the destabilized TTR^{L55P} protein, as previously described (39-42). Consistent with this, our LC-MS analysis of conditioned media showed that TTR^{L55P} levels were approximately 30% that of TTR^{WT} (**Fig. 2B**). This result mirrors the lower levels of destabilized TTR mutants, as compared to wild-type TTR, observed in conditioned media prepared on hepatic cells expressing both mutant and wild-type TTR and subjected to ATF6 activation (39-42).

Interestingly, since UPR signaling declines during normal aging, the presence of adaptive UPR signaling in these HLCs could reflect a protective biologic pathway whose activity also declines during the aging process. Aging-dependent reductions in adaptive UPR signaling could exacerbate TTR^{L55P}-associated ER stress and increase secretion

of TTR in non-native conformations that facilitate toxic extracellular aggregation. Thus, monitoring changes in hepatic UPR activation and/or conformational stability of circulating TTR tetramers could reflect a viable biomarker to monitor progression of TTR amyloid disease pathogenesis.

Concluding Remarks.

Our establishment of a universal gene correction strategy for TTR in iPSCs offers a unique opportunity to both demonstrate the broad therapeutic potential for this approach to ameliorate peripheral toxicity of secreted TTR associated with ATTR disease and identify new potential hepatic modifiers of disease pathogenesis (e.g., *TF* and UPR signaling). As we apply this strategy to diverse ATTR patient iPSC-derived HLCs, we will continue to refine our transcriptional analysis to define new potential biomarkers that can be translated to the clinic to improve diagnosis and treatment of this devastating disease.

METHODS

Details concerning experimental procedures are provided in the Supplemental Methods.

STATISTICAL ANALYSIS

Unless otherwise stated in the text, significance was determined between experimental and control conditions via unpaired Student's t-test. All experiments were performed using technical and biological triplicates. Here, we define biological replicates as being individual passages and/or separate differentiations. Additional statistical information can be found in individual figure legends.

AUTHOR CONTRIBUTIONS

RMG designed research studies, conducted experiments, acquired data, analyzed data, and wrote the manuscript. DCL designed research studies, conducted experiments, acquired data, analyzed data. TMM and NS analyzed data. JCJ conducted experiments. DNK, RLW, and GJM supervised and designed research studies, analyzed data, and revised the manuscript.

ACKNOWLEDGEMENTS

This work was supported by the National Institutes of Health - NIDDK (grant R01DK102635).

CONFLICT OF INTEREST

The authors have declared that no conflict of interest exists.

REFERENCES

1. Blancas-Mejia LM, and Ramirez-Alvarado M. Systemic amyloidoses. *Ann Rev Biochem*. 2013;82(745-74.
2. Buxbaum JN. The systemic amyloidoses. *Curr Opin Rheumatol*. 2004;16(1):67-75.
3. Merlini G, and Westermark P. The systemic amyloidoses: clearer understanding of the molecular mechanisms offers hope for more effective therapies. *J Intern Med.* 2004;255(2):159-78.
4. Wechalekar AD, Gillmore JD, and Hawkins PN. Systemic amyloidosis. *Lancet.* 2016;387(10038):2641-54.
5. Falk RH, Comenzo RL, and Skinner M. The systemic amyloidoses. *New Engl J Med.* 1997;337(13):898-909.
6. Reixach N, Deechongkit S, Jiang X, et al. Tissue damage in the amyloidoses: Transthyretin monomers and nonnative oligomers are the major cytotoxic species in tissue culture. *Proc Natl Acad Sci.* 2004;101(9):2817-22.
7. Ruberg FL, and Berk JL. Transthyretin (TTR) cardiac amyloidosis. *Circulation.* 2012;126(10):1286-300.
8. Benson MD. Pathogenesis of transthyretin amyloidosis. *Amyloid*. 2012;19 Suppl 1(14-5).
9. Ando Y, Nakamura M, and Araki S. Transthyretin-related familial amyloidotic polyneuropathy. *Arch Neurol.* 2005;62(7):1057-62.
10. Ericzon BG, Holmgren G, Lundgren E, et al. New structural information and update on liver transplantation in transthyretin-associated amyloidosis. Report from the 4th International Symposium on Familial Amyloidotic Polyneuropathy and Other

Transthyretin Related Disorders & the 3rd International Workshop on Liver Transplantation in Familial Amyloid Polyneuropathy, Umea Sweden, June 1999. *Amyloid*. 2000;7(2):145-7.

11. Genereux JC, Qu S, Zhou M, et al. Unfolded protein response-induced ERdj3 secretion links ER stress to extracellular proteostasis. *EMBO J*. 2015;34(1):4-19.
12. Gertz MA, Benson MD, Dyck PJ, et al. Diagnosis, Prognosis, and Therapy of Transthyretin Amyloidosis. *J Am Coll Cardiol*. 2015;66(21):2451-66.
13. Herlenius G, Wilczek HE, Larsson M, et al. Ten years of international experience with liver transplantation for familial amyloidotic polyneuropathy: results from the Familial Amyloidotic Polyneuropathy World Transplant Registry. *Transplantation.* 2004;77(1):64-71.
14. Hemming AW, Cattral MS, Chari RS, et al. Domino liver transplantation for familial amyloid polyneuropathy. *Liver Transpl*. 1998;4(3):236-8.
15. Llado L, Baliellas C, Casasnovas C, et al. Risk of transmission of systemic transthyretin amyloidosis after domino liver transplantation. *Liver Transpl.* 2010;16(12):1386-92.
16. Misumi Y, Narita Y, Oshima T, et al. Recipient aging accelerates acquired transthyretin amyloidosis after domino liver transplantation. *Liver Transpl.* 2016;22(5):656-64.
17. Muchtar E, Grogan M, Dasari S, et al. Acquired transthyretin amyloidosis after domino liver transplant: Phenotypic correlation, implication of liver retransplantation. *J Neurol Sci*. 2017;379(192-7).
18. Berk JL, Suhr OB, Obici L, et al. Repurposing diflunisal for familial amyloid polyneuropathy: a randomized clinical trial. *JAMA.* 2013;310(24):2658-67.
19. Ando Y, Sekijima Y, Obayashi K, et al. Effects of tafamidis treatment on transthyretin (TTR) stabilization, efficacy, and safety in Japanese patients with familial amyloid polyneuropathy (TTR-FAP) with Val30Met and non-Val30Met: A phase III, open-label study. *J Neurol Sci*. 2016;362(266-71.
20. Maurer MS, Elliott P, Merlini G, et al. Design and Rationale of the Phase 3 ATTR-ACT Clinical Trial (Tafamidis in Transthyretin Cardiomyopathy Clinical Trial). *Circ Heart Fail*. 2017;10(6).
21. Butler JS, Chan A, Costelha S, et al. Preclinical evaluation of RNAi as a treatment for transthyretin-mediated amyloidosis. *Amyloid.* 2016;23(2):109-18.

22. Meng Q, Zhuang Y, Ying Z, et al. Traumatic Brain Injury Induces Genome-Wide Transcriptomic, Methylomic, and Network Perturbations in Brain and Blood Predicting Neurological Disorders. *EBioMedicine.* 2017;16(184-94.
23. Prudencio M, Belzil VV, and Batra R. Distinct brain transcriptome profiles in C9orf72-associated and sporadic ALS. *Nat Neurosci.* 2015;18(8):1175-82.
24. Li X, Masliah E, Reixach N, et al. Neuronal production of transthyretin in human and murine Alzheimer's disease: is it protective? *J Neurosci*. 2011;31(35):12483-90.
25. Hawkins PN, Ando Y, Dispenzeri A, et al. Evolving landscape in the management of transthyretin amyloidosis. *Ann Med.* 2015;47(8):625-38.
26. Ando Y, Coelho T, Berk JL, et al. Guideline of transthyretin-related hereditary amyloidosis for clinicians. *Orphanet J Rare Dis.* 2013;8(31).
27. Leung A, Nah SK, Reid W, et al. Induced pluripotent stem cell modeling of multisystemic, hereditary transthyretin amyloidosis. *Stem Cell Reports*. 2013;1(5):451-63.
28. Leung A, and Murphy GJ. Multisystemic Disease Modeling of Liver-Derived Protein Folding Disorders Using Induced Pluripotent Stem Cells (iPSCs). *Methods Mol Biol.* 2016;1353(261-70.
29. Buxbaum JN. Animal models of human amyloidoses: are transgenic mice worth the time and trouble? *FEBS Lett.* 2009;583(16):2663-73.
30. Sousa MM, Fernandes R, Palha JA, et al. Evidence for early cytotoxic aggregates in transgenic mice for human transthyretin Leu55Pro. *Am J Pathol.* 2002;161(5):1935-48.
31. Wilson AA, Ying L, Liesa M, et al. Emergence of a stage-dependent human liver disease signature with directed differentiation of alpha-1 antitrypsin-deficient iPS cells. *Stem Cell Reports*. 2015;4(5):873-875.
32. Szkolnicka D, Hay DC. Concise Review: Advances in Generating Hepatocytes from Pluripotent Stem Cells for Translational Medicine. *Stem Cells*. 2016;34(6):1421-1426.
33. Bittencourt PL, Couto CA, Leitao RM, et al. No evidence of de novo amyloidosis in recipients of domino liver transplantation: 12 to 40 (mean 24) month follow-up. *Amyloid*. 2002;9(3):194-6.
34. Yamamoto S, Wilczek HE, Iwata T, et al. Long-term consequences of domino liver transplantation using familial amyloidotic polyneuropathy grafts. *Transpl Int*.

2007;20(11):926-33.

35. Stangou AJ, Heaton ND, and Hawkins PN. Transmission of systemic transthyretin amyloidosis by means of domino liver transplantation. *NEJM*. 2005;352(22):2356.
36. Ericzon BG. Domino transplantation using livers from patients with familial amyloidotic polyneuropathy: should we halt? *Liver Transpl*. 2007;13(2):185-7.
37. Buxbaum JN, Tagoe C, Gallo G, et al. Why are some amyloidoses systemic? Does hepatic “chaperoning at a distance” prevent cardiac deposition in a transgenic model of human senile systemic (transthyretin) amyloidosis? *FASEB J*. 2012;26(6):2283-2293. doi:10.1096/fj.11-189571.
38. Chen JJ, Genereux JC, Suh EH, et al. Endoplasmic Reticulum Proteostasis Influences the Oligomeric State of an Amyloidogenic Protein Secreted from Mammalian Cells. *Cell Chem Biol*. 2016;23(10):1282-93.
39. Chen JJ, Genereux JC, Qu S, et al. ATF6 activation reduces the secretion and extracellular aggregation of destabilized variants of an amyloidogenic protein. *Chem Biol*. 2014;21(11):1564-74.
40. Genereux JC, Qu S, Zhou M, et al. Unfolded protein response-induced ERdj3 secretion links ER stress to extracellular proteostasis. *EMBO J*. 2015;34(1):4-19.
41. Plate L, Cooley CB, Chen JJ, et al. Small molecule proteostasis regulators that reprogram the ER to reduce extracellular protein aggregation. *Elife*. 2016;5.
42. Shoulders MD, Ryno LM, Genereux JC, et al. Stress-independent activation of XBP1s and/or ATF6 reveals three functionally diverse ER proteostasis environments. *Cell Rep*. 2013;3(4):1279-92.
43. Loeffler DA, Connor JR, Juneau PL, et al. Transferrin and iron in normal, Alzheimer's disease, and Parkinson's disease brain regions. *J Neurochem.* 1995;65(2):710-24.
44. Raditsis AV, Milojevic J, Melacini G. A*β* Association Inhibition by Transferrin. *Biophys J*. 2013;105(2):473-480. doi:10.1016/j.bpj.2013.03.065.
45. Giunta S, Galeazzi R, Valli MB, et al. Transferrin neutralization of amyloid beta 25-35 cytotoxicity. *Clin Chim Acta.*2004;350(1-2):129-36.
46. Bloomer SA, Brown KE, Buettner GR, et al. Dysregulation of hepatic iron with aging: implications for heat stress-induced oxidative liver injury. *Am J Physiol Regul Integr Comp Physiol.* 2008;294(4):R1165-74.

47. Cook CI, and Yu BP. Iron accumulation in aging: modulation by dietary restriction. *Mech Ageing Dev.* 1998;102(1):1-13.
48. Jung SH, DeRuisseau LR, Kavazis AN, et al. Plantaris muscle of aged rats demonstrates iron accumulation and altered expression of iron regulation proteins. *Exp physiol.* 2008;93(3):407-14.
49. Ohta M, Sugano A, Hatano N, et al. Co-precipitation molecules hemopexin and transferrin may be key molecules for fibrillogenesis in TTR V30M amyloidogenesis. *Transgenic Res*. 2018;27(1):15-23. doi:10.1007/s11248-017-0054-x.
50. Walter P, and Ron D. The unfolded protein response: from stress pathway to homeostatic regulation. *Science.* 2011;334(6059):1081-6.
51. Hetz C, Chevet E, and Oakes SA. Proteostasis control by the unfolded protein response. *Nat Cell Biol.* 2015;17(7):829-38.
52. Lu PD, Jousse C, Marciniak SJ, et al. Cytoprotection by pre-emptive conditional phosphorylation of translation initiation factor 2. *EMBO J.* 2004;23(1):169-79.

FIGURE LEGENDS

FIGURE 1. Creation of a TTR promoter-driven hepatic specification reporter iPSC line and universal gene editing strategy for hereditary amyloidosis.

(A) Undifferentiated PSCs and day 24 HLCs (green and yellow columns, respectively) form distinct, independent clusters by microarray analysis. Top 10 differentially expressed upregulated in HLCs labeled on the y-axis, highlighted by green box. Top 10 genes upregulated in undifferentiated PSCs labeled on the y-axis (below). Top differentially expressed genes were determined by one-way ANOVA. (B) qRT-PCR validating microarray finding that expression of *TTR* mRNA is significantly upregulated in specified HLCs compared to undifferentiated iPSCs; fold-change calculated over undifferentiated iPSCs (n=3, *$p<0.05$, unpaired t-test for significance, bars denote standard deviation). (C) Schematic representation of the gene targeting strategy. Black triangles flank Cre-excisable LoxP sites. (D) Flow cytometry-based time course of GFP^+ (i.e. TTR^+) cells that appear throughout hepatic specification of targeted iPSCs (n=3, bars denote standard deviation). (E) Phase (left) and fluorescence (middle, right) microscopy images of day 26 reporter iPSC-derived HLCs. Images taken at 20X magnification. (F) Enrichment of hepatic markers in sorted day 16 TTR-GFP^+ HLCs;

fold-change calculated over undifferentiated iPSCs (n=5, bars denote standard deviation).

FIGURE 2. Gene-edited iPSC-derived HLCs no longer produce neurotoxic, destabilized TTR variants.

(A) Experimental overview depicting interrogation of corrected, uncorrected, and wild-type iPSC-derived HLC supernatants and determination of their requisite downstream effects on neuronal target cells. (B) Mass spectrometric (MS) analyses of supernatant from wild-type, uncorrected, and corrected iPSC-derived HLCs. Red trace: TTR^{WT}, pink trace: destabilized TTR^{L55P} variant. Bovine TTR (green) is an artifact of culture conditions. The molecular weight of each species is denoted in daltons. (C) SH-SY5Y cells were dosed for 7 days with conditioned iPSC HLC-derived supernatant from wild-type, uncorrected, or corrected conditions. Neuronal cell viability was determined via PI staining (n=3, unpaired t-test for significance comparing uncorrected and corrected conditions, bars denote standard deviation).

FIGURE 3. Single cell RNA sequencing (scRNAseq) of corrected vs. uncorrected syngeneic iPSC-derived HLCs reveals a novel hepatic gene signature.

(A) Experimental schematic for the transcriptomic comparison of corrected vs. uncorrected syngeneic iPSC-derived HLCs at day 16 of the hepatic specification protocol. (B) Uncorrected (red) and corrected (green) populations cluster independently by supervised principal component analysis (PCA). (C) Heatmap depicting the 92 genes differentially expressed between uncorrected and corrected populations. Columns represent individual cells, green bar denotes corrected cells, red bar denotes uncorrected cells. Rows represent differentially expressed genes. The top 10 genes as well proteostasis factor *EDEM2* are highlighted on the y-axis as determined via one-way ANOVA. Boxes represent distinct transcriptional signatures specific to uncorrected (red) and corrected (green) cells. (D) Violin plots representing relative expression levels of *TTR*, potential mediators of TTR fibrillogenesis (*TF*), and UPR target genes (*HYOU1, EDEM2*). (False discovery rate (FDR) determined via one-way ANOVA, *FDR<0.05, **FDR<0.005, ***FDR<0.0005.) (E) GSEA depicting significant enrichment of adaptive

UPR machinery (ATF6, XBP1s) but not PERK target genes in uncorrected HLCs. In these analyses, 100 uncorrected and 60 corrected cells were studied.

SUPPLEMENTAL FIGURE 1. Validation of targeted iPSC reporter line for site-specific integration of transgene as well as karyotypic stability. (A) Targeting construct used to perform gene correction. Red arrows denote the forward primer utilized for allele integration and puromycin cassette excision assay. Blue arrow represents the reverse primer used in the targeted integration screen. Green arrow depicts the reverse primer utilized for puromycin resistance ($puro^R$) cassette excision. (B) PCR screen of gDNA for targeted integration of donor construct (left) and excision of $puro^R$ cassette (right). (C) Non-targeted (left) and corrected (right) TTR^{L55P} iPSCs derived from a female ATTR amyloidosis patient were karyotypically normal, post-excision of the $puro^R$ cassette.

SUPPLEMENTAL FIGURE 2. Liver markers are not differentially expressed between uncorrected and corrected HLCs at day 16 of differentiation. Violin plots representing equivalent relative expression levels of genes known to be upregulated during hepatic specification of PSCs in uncorrected (red) and corrected (green) HLCs. None of the noted genes are differentially expressed between the two groups, suggesting competent normalization of the hepatic specification procedure.

Figure 1

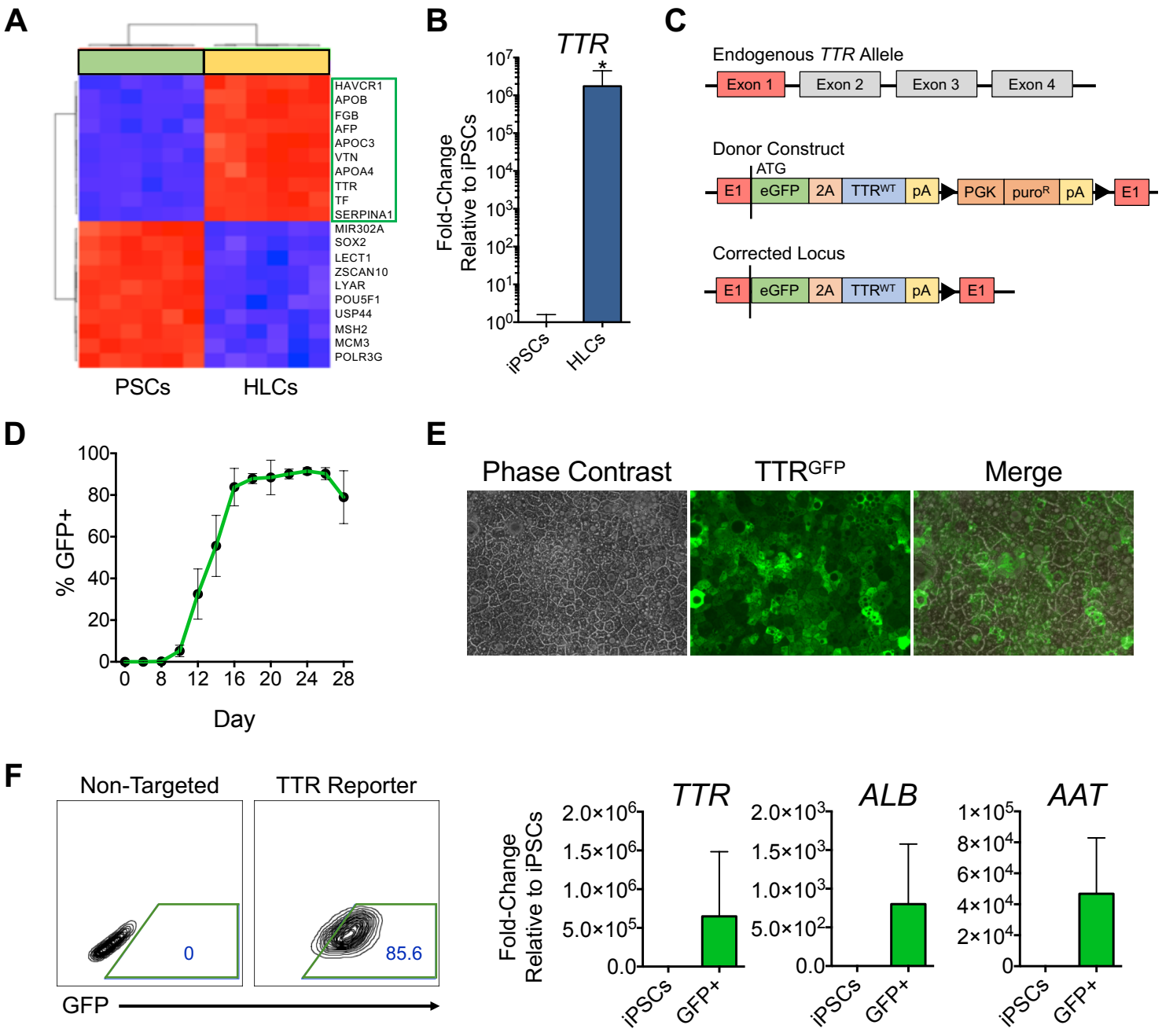
A
HAVCR1
APOB
FGB
AFP
APOC3
VTN
APOA4
TTR
TF
SERPINA1
MIR302A
SOX2
LECT1
ZSCAN10
LYAR
POU5F1
USP44
MSH2
MCM3
POLR3G
PSCs
HLCs
B
TTR
Fold-Change Relative to iPSCs
iPSCs
HLCs
C
Endogenous TTR Allele
Exon 1
Exon 2
Exon 3
Exon 4
Donor Construct
ATG
E1
eGFP
2A
TTRWT
pA
PGK
puroR
pA
E1
Corrected Locus
E1
eGFP
2A
TTRWT
pA
E1
D
% GFP+
Day
E
Phase Contrast
TTRGFP
Merge
F
Non-Targeted
TTR Reporter
0
85.6
GFP
TTR
ALB
AAT
Fold-Change Relative to iPSCs
iPSCs
GFP+

Figure 2

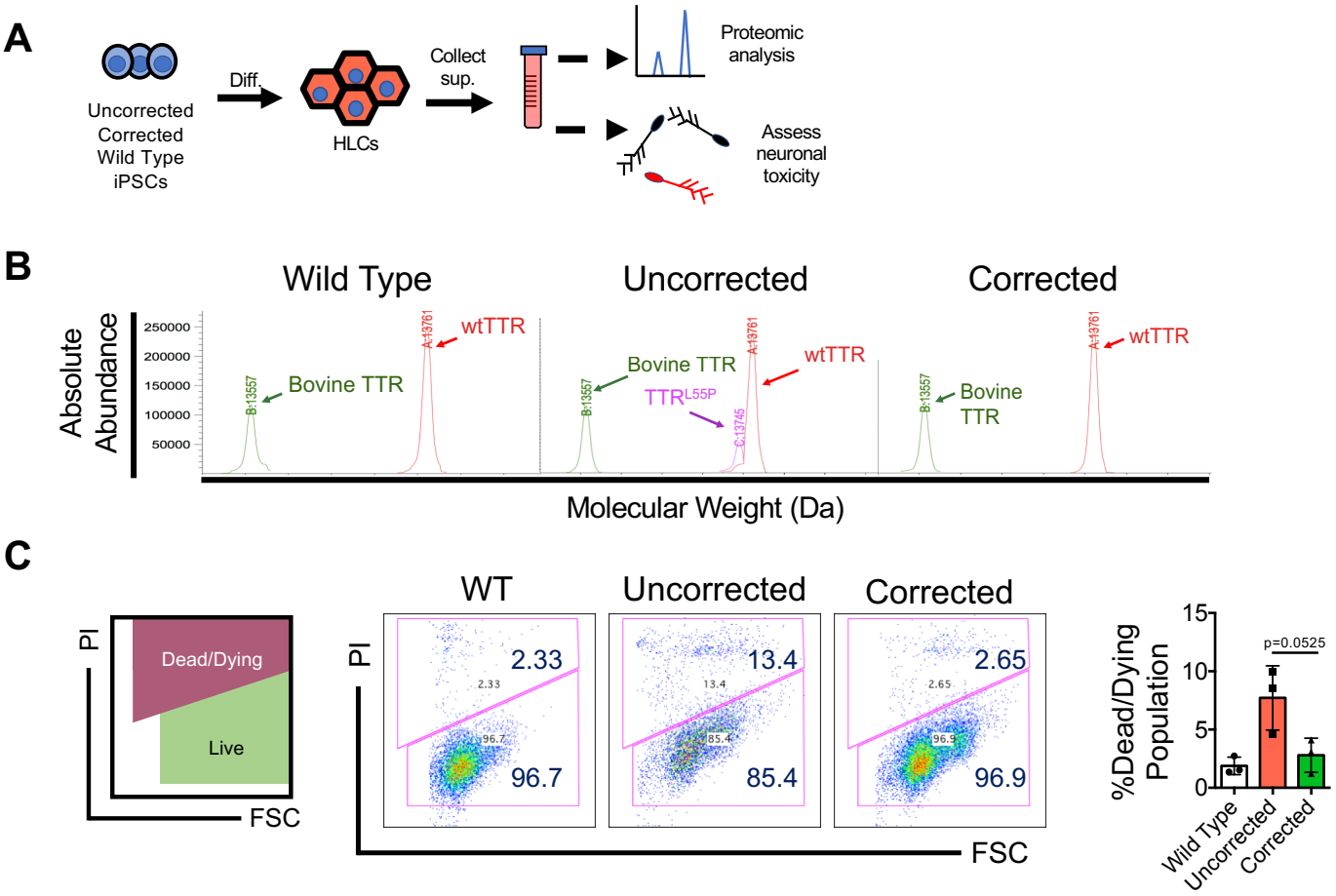
A
Uncorrected
Corrected
Wild Type
iPSCs
Diff.
HLCs
Collect
sup.
Proteomic
analysis
Assess
neuronal
toxicity
B
Wild Type
Uncorrected
Corrected
Absolute
Abundance
250000
200000
150000
100000
50000
B-13557
Bovine TTR
A-13761
wtTTR
Bovine TTR
TTRL55P
C-13745
wtTTR
Bovine
TTR
Molecular Weight (Da)
C
PI
Dead/Dying
Live
FSC
WT
Uncorrected
Corrected
2.33
96.7
13.4
85.4
2.65
96.9
%Dead/Dying
Population
15
10
5
0
p=0.0525
Wild Type
Uncorrected
Corrected

Figure 3

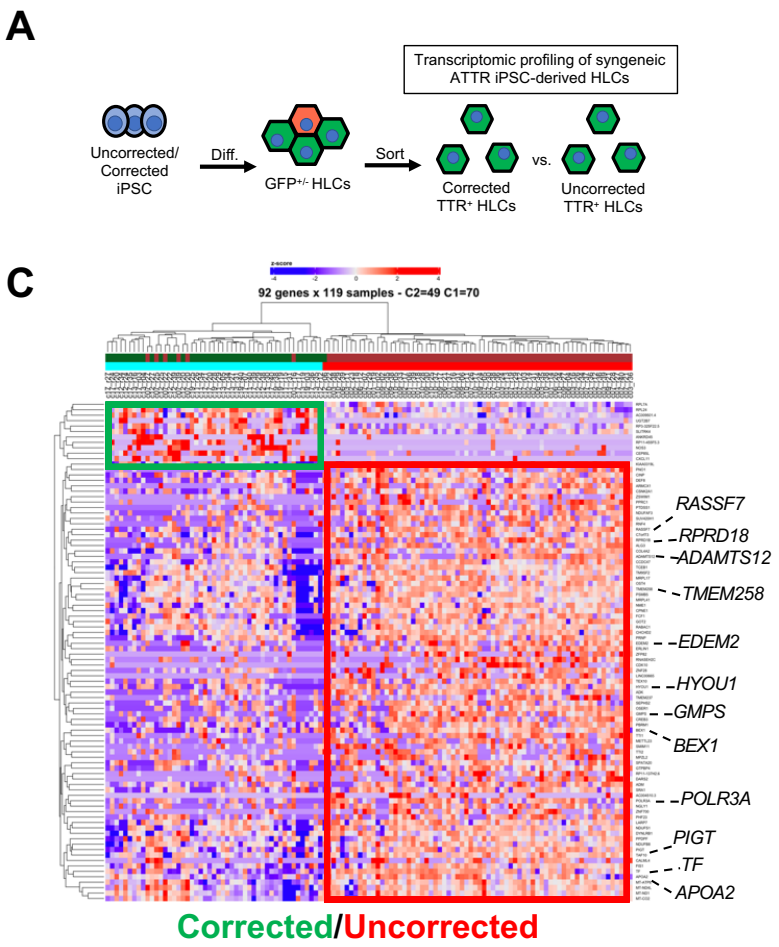

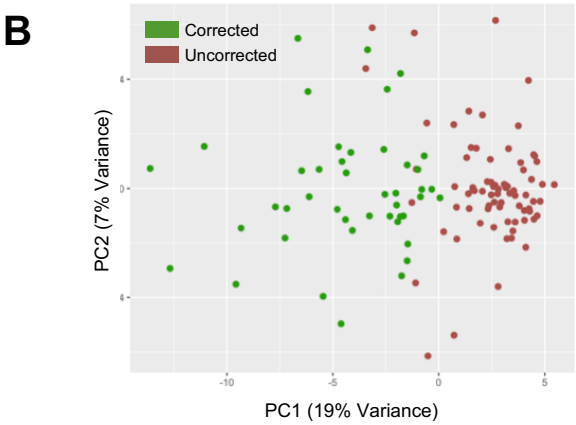

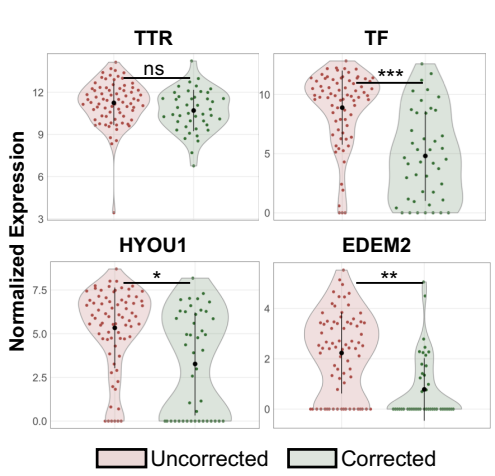

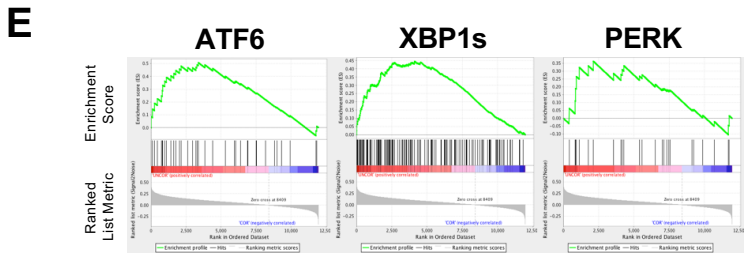

Gene Set	ATF6	XBP1s	PERK
FDR	0.035	0.029	0.314

Supplemental Figure 1

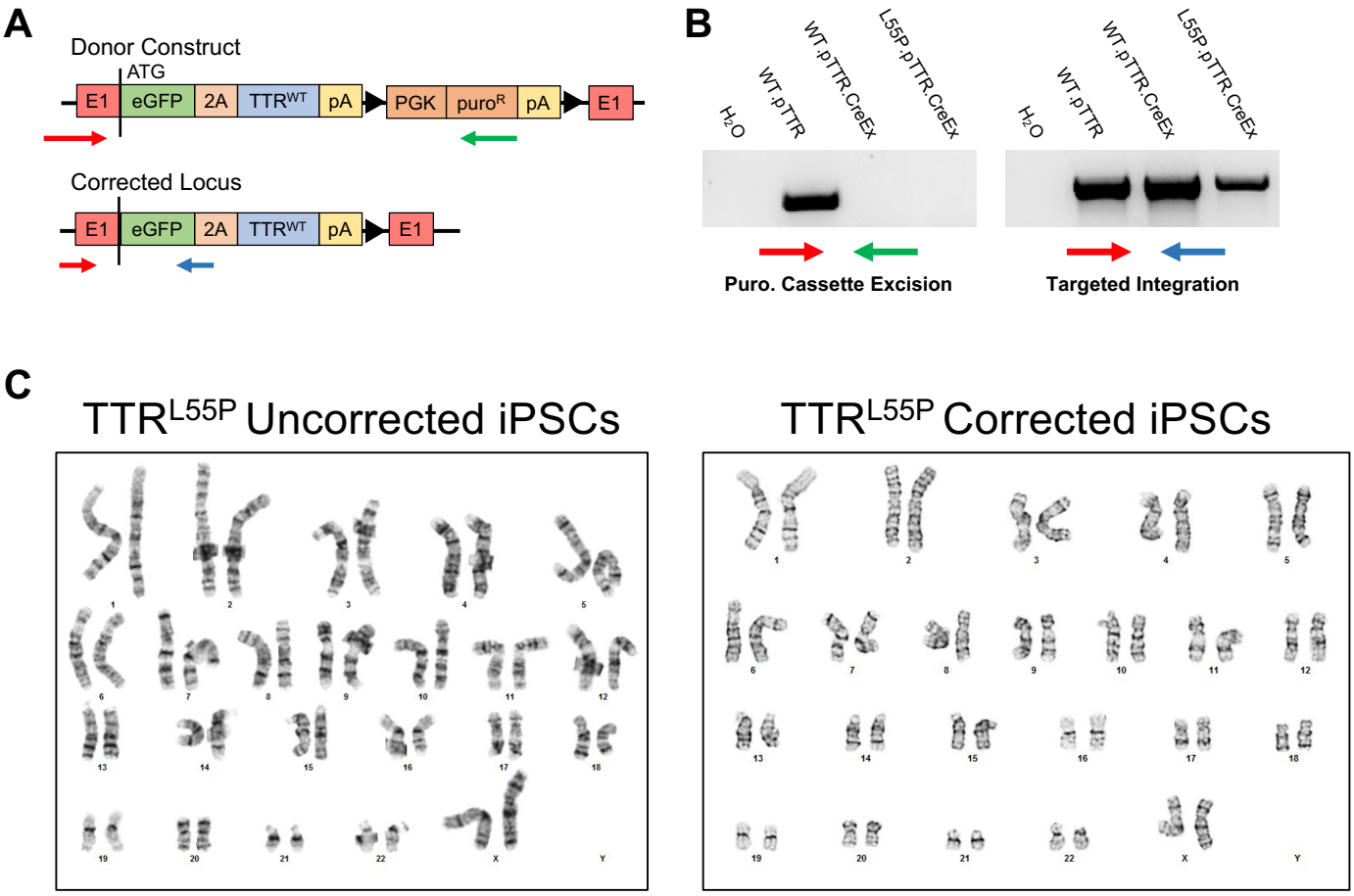
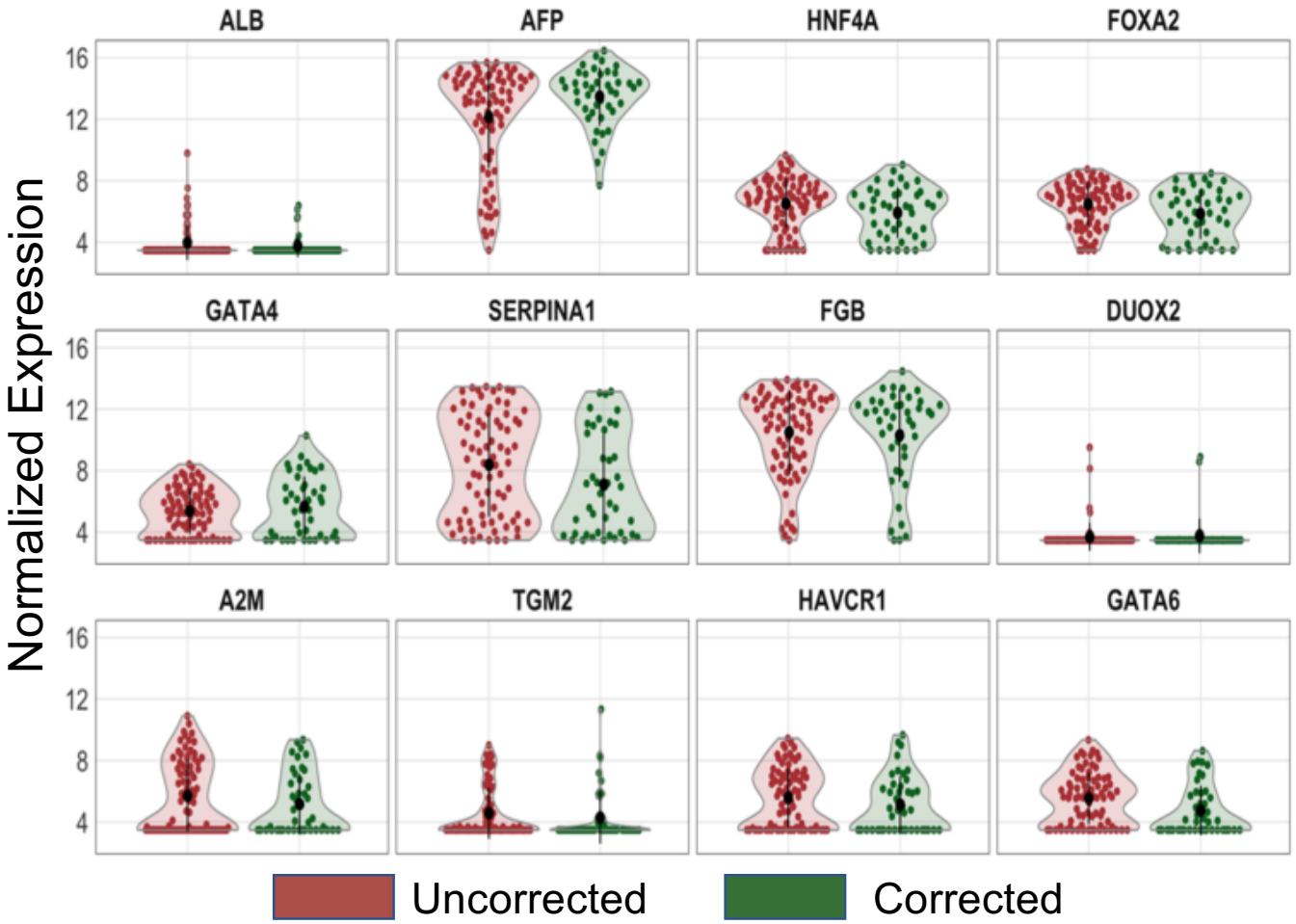
Supplemental Figure 2